Food & Function

Dynamic Article Links

Cite this: *Food Funct.*, 2012, **3**, 1206

www.rsc.org/foodfunction

PAPER

In vitro study of triglyceride lipolysis and phase distribution of the reaction products and cholesterol: effects of calcium and bicarbonate†

Zahari Vinarov,[a] Liliya Petrova,[a] Slavka Tcholakova,*[a] Nikolai Denkov Denkov,[a] Simeon D. Stoyanov[bcd] and Alex Lips[e]

Received 5th April 2012, Accepted 20th July 2012
DOI: 10.1039/c2fo30085k

We describe a relatively simple *in vitro* model for triglyceride (TG) lipolysis which mimics closely the conditions in the human stomach and small intestine. The main model advantages are: (1) as *in vivo*, sodium bicarbonate is used for buffering; (2) the pH-profile in the small intestine is closely matched; (3) the experimental procedure does not include complex equipment. To test its performance, the proposed *in vitro* model is applied to quantify the effects of Ca^{2+}, pH, and bicarbonate on the degree of TG lipolysis and on the solubilization of the lipolysis products and cholesterol in the aqueous phase. We found that TG lipolysis passes through a shallow minimum at 3.5 mM Ca^{2+} when varying the calcium concentration between 1 and 11 mM, while the presence of bicarbonate and the increase of pH led to a higher degree of lipolysis. Centrifugation and filtration were used to separate the aqueous phase and to study the solubilisation of the lipophilic components in the aqueous phase. We found that the solubilized cholesterol increases linearly with the concentration of free fatty acids (FFA) which is evidence for co-solubilization of these two components in the bile micelles. At high Ca^{2+} concentrations, aggregates larger than 300 nm were observed by cryo-microscopy and light scattering, which solubilize well cholesterol and saturated FFA. In contrast, the monoglycerides were always predominantly solubilized in the small bile micelles with diameters around 4 nm.

1. Introduction

Lipid digestion in the gastro-intestinal tract (GIT) has been extensively studied, due to its importance for human health and for the food and pharmaceutical industries.[1–30] Due to ethical, social and health issues, *in vivo* human studies are difficult and expensive, and are usually limited to fecal sample analysis.[31–35] Therefore, numerous *in vitro* digestion models were developed which mimic the conditions in the GIT.[8,11,13,16,18,29–31,36–40]

Two types of *in vitro* models can be distinguished:[30] (1) single step models, where one particular region of the GIT is simulated, *e.g.*, mouth, stomach, small intestine, or colon; (2) multiple step models, where two or more compartments of the GIT are simulated.

The most sophisticated model of the second type is the TIM™ lipid absorption system, developed by TNO Quality of Life, The Netherlands.[17,18] In this system, four computer-controlled chambers simulate the dynamic physiological processes, which occur in the stomach, duodenum, jejunum and ileum for TIM-1, and also in the large intestine for TIM-2.[17,18,40] In this method, the pH-profile in the intestine is controlled by addition of bicarbonate, as it is *in vivo*. This system enables the removal of the digestion products, thus mimicking more closely the *in vivo* conditions. All these advantages come at the expense of using complex and costly machinery, which explains why this method is not widely used in research laboratories.[15]

The single step models usually apply a pH-titrator unit to maintain constant pH throughout the experiment.[30] This measurement consists of titrating the FFA which are liberated in the course of triglyceride lipolysis (TG lipolysis). A major advantage of this method is the possibility for rapid screening of the effects of food composition and structure on lipid digestibility. Due to its relatively simple procedure and non-expensive equipment, this "pH-stat" method is widely used in the research studies.[11,12,16,25,29,30,36,41–43] Most of these studies focus on determining the rate of FFA release under conditions close to those in the small intestine, where the main fat digestion occurs.[11,21,25,29,36,41–44] A comprehensive review of the main results obtained in these studies was presented recently by McClements and Li.[30]

[a]*Department of Chemical Engineering, Faculty of Chemistry and Pharmacy, Sofia University, 1 James Bourchier Ave., 1164 Sofia, Bulgaria. E-mail: SC@DCE.UNI-SOFIA.BG; Fax: +359-2 962 5643; Tel: +359-2 962 5310*
[b]*Unilever R&D, Vlaardingen 3133AT, The Netherlands*
[c]*Laboratory of Physical Chemistry and Colloid Science, Wageningen University, 6703 HB Wageningen, The Netherlands*
[d]*Department of Mechanical Engineering, University College London, Torrington Place, London WC1E 7JE, UK*
[e]*Unilever Discover, Port Sunlight Laboratory, Quarry Road East Bebington, CH63 3JW, Wirral, UK*
† Electronic supplementary information (ESI) available. See DOI: 10.1039/c2fo30085k

The accumulated results evidence[11,12,21,30,36,42,44] that the digestion rate depends strongly on the detailed composition of the reaction mixture – enzyme concentration,[44] presence of colipase,[21,45,46] bile concentration,[11,12,36] calcium concentration,[11,12,42] *etc.* For this reason, the *in vitro* models aiming to mimic the digestion process in the GIT, use complex mixtures of buffers, salts, enzymes, co-enzymes, bile salts, phospholipids and other components, in concentrations as close as possible to the *in vivo* conditions.[30]

Due to the specific principle of measurement (*viz.* titration of the formed FFA), in most of these *in vitro* studies[11,12,16,25,29,30,36,41–43] the pH is maintained or it is increased in a step-wise manner (*e.g.*, to mimic the transition from stomach to small intestine) by adding NaOH. However, the pH control *in vivo* is realized by secretion of bicarbonate ions with high buffering capacity.[47,48] No bicarbonate is added to the reaction mixture in most *in vitro* models,[11,12,16,25,29,30,36,41–43] because the buffering effect of the bicarbonate ions compromises the measurements of the formed FFA by the pH-stat method. On the other hand, the presence of bicarbonate in the reaction mixture can be important in many cases, *e.g.*, when the effects of calcium ions on the fat lipolysis and on the redistribution of the reaction product is studied, due to the strong interactions between Ca^{2+} and carbonate ions. Therefore, the lack of bicarbonate ions in such *in vitro* studies calls for some additional justification and verification of the obtained results and conclusions.

It is well known from *in vivo* experiments that the dairy calcium significantly affects the fat lipolysis and can reduce the body weight.[33–35] It was shown that the increase of calcium intake increases the total fat excretion, but does not affect the excretion of bile acids.[33] Interestingly, it was found that the high calcium diet significantly reduces the total and the LDL cholesterols, but does not affect the HDL cholesterol, which can be of potential benefit to human health.[34] As explained by Shahkhalili *et al.*, the mechanism by which calcium lowers the blood cholesterol still remains unclear.[35]

Several *in vitro* studies considered the effect of calcium on the initial rate of the lipolysis reaction and on the overall degree of lipolysis after certain periods of time.[11,42,49,50] However, calcium can also affect the type and the size of the formed aggregates (micelles, vesicles, precipitates) in the course of fat digestion and, as a consequence, to affect the bioavailability of the lipophilic substances in the mixture, such as cholesterol, FFA, and monoglycerides. As far as the transport through the mucus layer in the intestine is mainly diffusion controlled, the bioavailability of the lipophilic substances is controlled by the size and shape of the molecular aggregates (vesicles and micelles), in which these substances are solubilized. As shown with colloidal particles, only particles with sizes smaller than 0.5 μm have high ability to diffuse through the mucin layer.[51,52] Therefore, depending on the adhesive properties of the micelles and vesicles, the typical size of the aggregates which can penetrate the mucus layer and transport lipophilic substances is expected to be below *ca.* 0.5 μm.[53]

Based on the above literature overview, two major aims of the current study have been formulated: (1) to develop a relatively simple *in vitro* model which allows one to use a bicarbonate buffer for ensuring the appropriate pH profile of the reaction mixture. (2) By using this model to evaluate the effect of calcium on the degree of fat digestion and on the solubility of the lipolysis products and cholesterol in the aqueous phase, thus focusing on the mechanistic aspects of the calcium effects.

Two size ranges of the molecular aggregates are studied – aggregates with sizes below 200 nm, and those with sizes between 200 nm and 1 μm. Respectively, two methods were used for separation of the aqueous phase, containing such aggregates: filtration through 200 nm cut-off filter and centrifugation. Gas chromatography (GC) and thin layer chromatography (TLC) were used to determine the overall degree of fat lipolysis and the concentrations of the monoglycerides, diglycerides (DG), triglycerides, free fatty acids and cholesterol, solubilized in the aqueous phase. The aqueous phase was analyzed also by atomic absorption spectrometry (AAS) to determine the concentration of soluble Ca^{2+} ions. To characterize the size and morphology of the molecular aggregates, we used dynamic light scattering (DLS) and transmission electron cryo-microscopy (cryo-TEM).

The article is organized as follows: the used materials and methods are described in Section 2. Section 3.1 compares the *in vitro* conditions of the newly proposed lipolysis model with the conditions in the human stomach and small intestine. In Section 3.2 we present data for the effect of Ca^{2+} concentration on the TG hydrolysis, in the presence and in the absence of bicarbonate. Section 3.3 describes results for the effect of pH profile on TG hydrolysis. Section 3.4 describes the effect of Ca^{2+} on the distribution of the reaction products and cholesterol in the aqueous phase, as obtained after filtration or centrifugation of the reaction mixture. The main conclusions are summarized in Section 4. Note that the methods described in subsections 2.3, 2.4 and 2.7 involve significant original elements, whereas the remaining subsections in Section 2 describe procedures known from the literature, with possible minor modifications.

2. Materials and methods

2.1. Materials

We used commercial sunflower oil (SFO) bought from a grocery store in Bulgaria. This SFO was purified by multiple passes through a chromatography column filled with Florisil adsorbent, until the interfacial tension with pure water became ≈ 32 mN m^{-1}, which is an indication of the removal of all polar contaminants.[54]

Pancreatin from porcine pancreas (Sigma-Aldrich, cat. no. P8096), containing a range of enzymes including amylase, trypsin, lipase, ribonuclease and protease, was used as a source of pancreatic lipase and colipase (at 1 : 1 molar ratio in the pancreatic source[55,56]). The lot numbers of the used pancreatin samples were 088K0764 and 087K1888. According to the producer, both lots possessed an activity of 4.9 USP units per mg, defined as follows: pancreatin releases 4.9 microequivalents of fatty acids per min per mg pancreatin from olive oil at pH = 9.0 at 37 °C.

Pepsin from porcine gastric mucosa (Fluka, cat. no. 77160), with lot number 1238420, was used. The activity of this pepsin is 643 U mg^{-1}. One unit here corresponds to the amount of enzyme, which increases the absorbance at 280 nm by 0.001 per minute at pH = 2.0 and 37 °C, using hemoglobin as the substrate.

As a source of bile salts we used porcine bile extract, obtained from Sigma-Aldrich (cat. no. B-8631, lots no. 038K0014, 119K0048, 050M0133, 100M0192V, 031M0106V). This extract contains 50 wt% bile acids, 6 wt% phosphatidylcholine and less

than 0.06 wt% Ca^{2+}.[11] Our analysis by gas chromatography showed also the presence of 1.8 wt% cholesterol and 4.3 wt% fatty acids. According to the producer, the composition of the bile salts in this extract is 13 wt% hyodeoxycholic acid, 18 wt% deoxycholic acid, 5 wt% cholic acid, 39 wt% glycodeoxycholic acid, and 24 wt% taurodeoxycholic acid. The percentages of these bile acids and the corresponding molecular masses were used to calculate an average molecular mass of 442 g mol^{-1} – the latter was used to define the average molar concentration of bile salts in our experiments.

For the preparation of the electrolyte solutions, we used NaCl (product of Merck), KCl (product of Merck), $CaCl_2$ (product of Fluka) and $NaHCO_3$ (product of Teokom), all of purity higher than 99%.

The standards used for determination of the retention times in GC and the retention factors in TLC were: myristic acid (98%, Fluka, cat. no. 70082), palmitic acid (98%, Riedel de Haen, cat. no. 27734), stearic acid (97%, Acros, cat. no. 174490025), oleic acid (85%, Tokyo Kasei Kogyo, cat. no. 00011), 2-oleyl glycerol (95%, Sigma, cat. no. M2787) and dipalmitin (99%, Sigma, cat. no. D2135), cholesterol (95%, Sigma, cat. no. 26740), and triolein (99%, Fluka, cat. no. 92859).

2.2. Procedure for emulsion preparation

Stock oil-in-water emulsions were prepared by stirring 20 mL emulsifier solution and 30 mL sunflower oil (60 vol% oil) for 5 min. The emulsifier solution contained 1 wt% Tween 80, 10 mM NaCl and 0.1 g L^{-1} NaN_3. A rotor-stator homogenizer Ultra Turrax T25 (Janke & Kunkel GmbH & Co, IKA-Labortechnik), operating at 13 500 rpm, was used for emulsification. The formed emulsions were stored in glass jars for no more than 1 week, at room temperature. Before usage, these stock emulsions were re-homogenized by gentle hand-shaking. For performing the actual lipolysis experiment, the necessary amount of the stock emulsion was taken by a pipette and diluted in the electrolyte-enzyme solutions, as explained in Sections 2.3 and 2.4.

The drop size distribution in these emulsions was determined by video-enhanced optical microscopy.[57,58] The oil drops were observed in transmitted light with microscope Axioplan (Zeiss, Germany), equipped with objective Epiplan ×50, and connected to CCD camera and video-recorder. The diameters of the recorded oil drops were measured using custom-made image analysis software. For each sample, the diameters of at least 1000 drops were measured. The accuracy of the optical measurements was estimated to be ±0.3 μm.[57]

The volume-surface diameter, d_{32}, characterizes the mean drop size in the studied emulsions and it was calculated from the relation:

$$d_{32} = \sum N_i d_i^3 / \sum N_i d_i^2 \quad (1)$$

where N_i is the number of drops with diameter d_i. All studied emulsions had $d_{32} = 20 \pm 3$ μm.

2.3. Lipolysis experiments in the presence of bicarbonate and calcium

It is a non-trivial task to reproduce the *in vivo* pH profile in the intestine. As mentioned above, the acidic content of the stomach is neutralized by bicarbonate which is secreted when the stomach juice enters the duodenum. The pH at this stage is around 5.5, increasing to a maximal value of pH = 7.5 during the passage through the jejunum and the ileum, which takes place for approximately 6 hours.[59]

In vitro, the pH of the gastric solution after neutralization with bicarbonate increases much more quickly: pH ≈ 8 is achieved after 1 hour of solution stirring in an open reaction vessel. Therefore, a special *in vitro* procedure is needed to slow down the increase of pH of the bicarbonate solutions. One possible way is to use the procedure developed by Miller *et al.*,[60] in which the bicarbonate in the system is slowly introduced using dialysis tubing. However, the focus of our study is on the lipolysis in the small intestine and that is why we increased the pH from 1.3 (gastric) to 5.5 (duodenal) by adding sodium bicarbonate directly to the reaction mixture. To ensure a gradual increase of pH from 5.5 to 7.5 in the appropriate time-scale, we slowed down the release of carbon dioxide from the reaction mixture, as explained below.

It is known that the process of acid neutralization by carbonates leads to formation of carbonic acid, which decomposes into water and carbon dioxide, and the latter is released as gas. This process could be slowed down by increasing the partial pressure of carbon dioxide gas above the reaction solution, thus shifting the chemical equilibrium toward higher concentrations of carbonic acid in the reaction mixture.[61] We achieved this goal by limiting the volume of the gas phase in the reaction vessel, so that the release of a relatively small amount of carbon dioxide from the solution was sufficient to increase its partial pressure above the solution and to slow down the carbonic acid decomposition and the related increase of pH. Technically, this procedure was realized as follows:

First, we prepared the following basic (stock) solutions: saline solution (59 mM NaCl + 35 mM KCl + 3.5 mM $CaCl_2$); pepsin solution (12.5 mg pepsin + 6.5 mL 0.25 M HCl, 5 min stirring at 37 °C); bile salts solution (375 mg bile extract + 5 mL H_2O, 30 min stirring at 37 °C); and pancreatic solution (30 mg pancreatin + 5 mL H_2O, 10 min stirring at 37 °C).

For preparation of all solutions we used deionized water from a water-purification system, Elix 3 (Millipore, USA). Saline, $CaCl_2$ and $NaHCO_3$ solutions were prepared and stored at room temperature. Before their mixing in the actual experiments, these solutions were thermostated at $T = 37$ °C. The pepsin, bile salts and pancreatic solutions were prepared directly at 37 °C, just before their use in the actual experiments.

The order of mixing of these solutions is schematically shown in Fig. 1. The solutions were mixed in bottles of 30 mL volume, which was essential to obtain the desired pH profile in the "intestinal" stage of the lipolysis experiment (see the explanations below). The bottles were kept closed during the lipolysis experiment, unless specified otherwise.

To start the lipolysis experiments, we first added 8.5 mL saline solution to 6.5 mL pepsin solution. In the experiments aimed at determining the effects of Ca^{2+}, here we added the required volume of 1 M $CaCl_2$ solution (between 0 and 300 μL). Afterwards, we added 200 μL of 60 vol% SFO emulsion in the saline + pepsine solution. The pH at this stage of the experiment was pH ≈ 1.3 and the solution was stirred for 30 min. Then, we carefully added 5 mL of 720 mM $NaHCO_3$ solution and homogenized the sample very gently by hand. Note that the

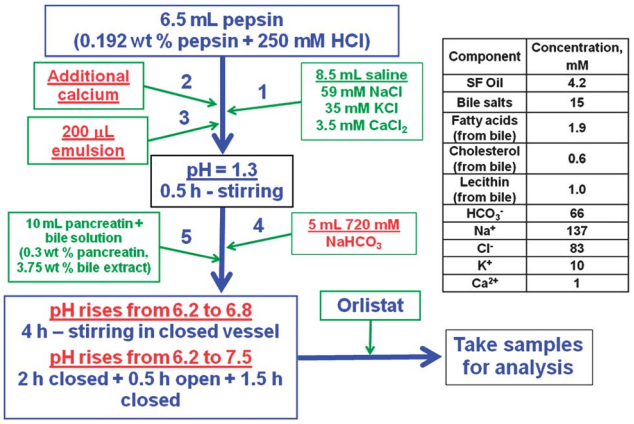

Component	Concentration, mM
SF Oil	4.2
Bile salts	15
Fatty acids (from bile)	1.9
Cholesterol (from bile)	0.6
Lecithin (from bile)	1.0
HCO_3^-	66
Na^+	137
Cl^-	83
K^+	10
Ca^{2+}	1

Fig. 1 Schematic presentation of the procedure for mixing the solutions and performing the lipolysis reaction in the *in vitro* test, performed in the presence of carbonate buffer. The inserted table shows the molar concentrations of the main components in the complete reaction mixture.

bicarbonate partially neutralizes the acidic solution at this point, producing CO_2, which can cause foaming and overflowing of the sample – the gentle hand-shaking allowed us to homogenize the sample without excessive foaming and overflow. Afterwards, we added 5 mL of 90 mM bile salts solution to 5 mL pancreatic solution (containing 0.6 wt% pancreatin), mixed them by hand, and added them to the reaction mixture, thus making its final volume equal to 30 mL.

The main components in the final reaction mixture are with the following concentrations: 4.2 mM sunflower oil (0.4 vol%), 15 mM bile salts, 0.1 wt% pancreatin, 0.0417 wt% pepsin, 1 mM Ca^{2+}, 10 mM K^+, 137 mM Na^+, 83 mM Cl^-, 66 mM HCO_3^-. These solutions contain also 0.6 mM cholesterol, 1 mM lecithin, and 1.9 mM fatty acids, which all originate from the bile extract.

It is important that during the addition of bicarbonate, bile salts and pancreatic solutions, the magnetic stirring is turned off. In this way, only a small fraction of CO_2 is released into the atmosphere and the pH at this stage is pH = 6.2 ± 0.1 (note that the equilibrium pH of a sodium bicarbonate solution is around pH = 8.5). Afterwards, we closed the bottles with the solution and turned on stirring. The solution started to release CO_2 and the pH in the mixture gradually increased. The rate of CO_2 release was reduced by minimizing the gas volume in the bottle (6.0 mL gas phase above 30 mL solution, with dimensions – height 1.5 cm, i.d. 2.25 cm) and by closing tightly the bottle cap. Thus we were able to control the pH profile of the mixture, without using a pH-stat instrument.

We performed experiments at two pH profiles. The first set of experiments was performed at pH values that increased gradually from 6.2 to 6.8, and this was achieved by stirring of the solution for 4 h in a closed bottle. In the second procedure, the pH was increased from 6.2 to 7.5 and this was achieved by stirring for 2 h in a closed bottle, then removal of the bottle cap and stirring for another 30 min in an open bottle (the pH raised from 6.5 to 7.4), finally closing the bottle again and stirring for additional 1.5 h (the pH reached 7.5).

After the end of the reaction time, which was 4 h for both procedures, we added 24 mg Orlistat granules (Xenical®, Roche) to inhibit the lipase action and stirred for 10 min. Afterwards the oil soluble components in the sample were extracted with chloroform or the sample was filtrated/centrifuged to obtain a clear aqueous phase for analysis.

2.4. pH-dynamic procedure

An alternative procedure was designed to mimic the pH profile described in the previous section, however, by using pH-STAT apparatus instead of bicarbonate to control the pH (note that the titration of the released fatty acids by the pH-stat instrument cannot be performed in the presence of high concentrations of buffer). We used the same solutions as described in the previous section and the concentrations of the different components in the final reaction mixture were similar to those shown in Table 1. The only exception was the bicarbonate, which was replaced by NaCl to create a similar concentration of Na^+ ions in the reaction mixture. For brevity, we will call this procedure "pH-dynamic", because of the pH changes throughout the experiment.

The order of mixing of the solutions is schematically shown in Fig. S1 (see the ESI†). First, we added 8.5 mL saline solution to 6.5 mL pepsin solution. In the experiments aimed at determining the effect of Ca^{2+}, here we added the required volume of 1 M $CaCl_2$. Afterwards, we added 200 µL of 60 vol% SFO emulsion. The pH at this stage of the experiment is pH = 1.3 and the solution was stirred for 30 min. Then, we adjusted the pH to 6.4 with ~500 µL of 3 M NaOH and added 1 mL of 2 M NaCl solution. Thus we ensured the same ionic strength, as in the experiments with $NaHCO_3$. Afterwards we added 5 mL of 90 mM bile salts solution to 5 mL pancreatic solution (0.6 wt% pancreatin), mixed them by hand, and added to the reaction mixture. Then, we fixed the pH to pH = 6.5 with the pH-STAT program and the solution was stirred for 2.5 h. Afterwards, the pH-STAT apparatus was set to increase the pH gradually from 6.5 to 7.4 for 30 min. Finally, a pH-STAT programme at pH = 7.5 was started and the solution was stirred for an additional 1 h. After the end of the reaction period (4 h, as in the presence of bicarbonate), we added 24 mg Orlistat granules and stirred for 10 min to block the lipolysis. Finally extraction with chloroform, or filtration/centrifugation was used to separate the aqueous phase.

Note that around 6.5 mL of NaOH were dispensed while increasing the pH from 6.5 to 7.4 by the pH-STAT instrument. To compensate partially for the increase of the solution volume during titration, the initial volume of the reaction mixture before titration was designed to be 26.5 mL in this procedure, *i.e.* around 10% smaller than that in the presence of bicarbonate (30 mL). During the increase of pH, this volume gradually increased up to 33 mL. Thus, on average, the volume of the reaction mixture was approximately the same in the two procedures to be compared (with carbonate and in the pH-dynamic procedure).

The pH-STAT apparatus is a product of Metrohm, Switzerland. The controlling module is Titrando 842 and the dosing device is Dosino 800. The pH electrodes are Ecotrode Plus and Unitrode, products of Metrohm. The STAT regimes were carried out at a titration rate of 50 µL min^{-1}. The titrant was 25 mM NaOH solution, which was standardized by titrating to an

Table 1 Comparison of the concentrations of the main components in the stomach and in the small intestine, as determined *in vivo*, with those in our *in vitro* model with carbonate buffer (see also Fig. 1)

		Concentration, mM				
Compartment		Ca^{2+}	Na^+	K^+	HCO_3^-	Bile salts
Stomach	*In vivo*	0.6 (ref. 67)	11–68 (ref. 66–69)	14–17 (ref. 67–69)	0	0 (ref. 67)
	In vitro	2	33	20	0	0
Small intestine	*In vivo*	0.5–1 (ref. 67 and 70)	140–150 (ref. 66, 67 and 71–73)	4.5–10 (ref. 67 and 71–73)	110–150 (ref. 73–75)	10–15 (ref. 6 and 76–79)
	In vitro	1	136	10	120	15

endpoint of pH = 7 with a fresh solution of potassium hydrogen phthalate ($KHC_8H_4O_4$) of known concentration.

2.5. Phase separation methods

(A) Filtration. The reaction mixture was first filtered through filter paper with a pore size of 2–3 μm and a weight of 84 g m^{-2} (BOECO, Germany). The filtration was carried out in a glass funnel and the filtrate was collected in a glass flask. Afterwards the obtained permeate was further filtered through a 200 nm filter Minisart NY25 (Sartorius, Germany) by syringe. The obtained permeate was clear and was then subjected to chloroform extraction, as described in Section 2.6. All filtration operations were performed at 37 °C.

(B) Centrifugation. The reaction mixture was centrifuged for 1 h at 3622*g* (4500 rpm) in a SIGMA 3-16PK centrifuge, at 37 °C. Afterwards, the serum was carefully withdrawn by syringe and the lipophilic substances in it were extracted with chloroform.

2.6. Extraction of the non-hydrolyzed TG and reaction products by chloroform

After stopping the lipolysis reaction with Orlistat granules, the reaction mixture was allowed to cool to room temperature and its pH was decreased to pH = 2 by adding HCl (to decrease the solubility of the reaction products in the aqueous phase). Next, 6 mL chloroform was added and the sample was sonicated for 15 min. After every 5 min of sonication, the sample was agitated by vigorous hand shaking. The obtained complex dispersion was centrifuged for 30 min at 3622*g* (4500 rpm), which led to separation of clear aqueous and organic phases, indicating that the oily drops were entirely transferred into the chloroform phase.

The same extraction procedure was applied to the clear aqueous phases, separated by filtration or centrifugation – see Section 2.5. The obtained chloroform phase was further analyzed by TLC and GC.

2.7. Thin layer chromatography (TLC)

TLC was used to determine the concentration of the triglyceride remaining after completion of the pancreatic lipolysis.

We used aluminium backed Silicagel 60 F 254 plates, with 20 × 20 cm^2 dimensions. The start line was drawn 2 cm from the plate bottom. The start–front distance was 15 cm. The samples were deposited on the plate with 5 μL capillaries, at 1.5 cm distance from each other. As a carrier liquid phase we used the mixture petroleum ether (product of Merck, cat. no. 1.01775.5000), diethyl ether (product of Merck, cat. no. 1.00921.100), and acetic acid (product of Teokom), in a 80 : 20 : 1 ratio by volume. The depth of the carrier liquid in the chamber was below 1.5 cm and the chromatography chamber was pre-saturated with vapours of the carrier liquid for 15 min before introducing the TLC plate into it. After the carrier liquid had reached the front line, the plate was taken out of the chamber and left to dry for 15 min.

The plate was then dipped for 1–2 s in a 6 wt% phosphomolybdic acid (product of Riedel de Haen, cat. no. 31426) dissolved in *i*-propanol, dried for 15 min, and heated to 100 °C for 15 min to visualize the spots of the separated components.[62] During heating, the phosphomolybdic acid reacts with the lipids, forming "molybdenum blue" spots. This procedure allowed us to observe the spots corresponding to triglycerides, diglycerides, monoglycerides, unsaturated free fatty acids and cholesterol. The different peaks were identified using the standard substances, described in Section 2.1.

To quantify the spot intensity, the TLC chromatograms were scanned by a scanner "Epson Perfection V100", with a resolution of 600 dpi. The scanned image was converted to grayscale by using Corel Photo Paint 12 or Photoshop CS2. The obtained image was digitally inverted, so that the spots appear bright on the dark background, and exported as a tif-file. Afterwards, this file was imported into custom-made software for image analysis, which allows the determination of peak intensity, I, as a function of the vertical position, y, in a rectangle covering the analyzed lane in the chromatogram. More precisely, the software determines the mean intensity as a function of the vertical position, in each lane of the chromatogram.

To determine the peak areas, we fitted each peak using a Gaussian curve and calculated the areas from the best fit parameters. To determine the concentration of the analyzed components, we constructed calibration curves which showed that the peak area and concentration were related by power–law dependence:

$$A_P(C) = A_{P0}C^n \quad (2)$$

The power–law index, $n = 0.49$, was determined for the triglyceride. The value of the pre-factor A_{P0} depended on the specific experimental conditions during chromatogram visualization (temperature, concentration of phosphomolybdic acid, *etc.*). Therefore, A_{P0} was determined using an internal standard of known concentration for each chromatogram. In this way, using the values of n and A_{P0}, we determined the concentration of the substance that had created a given peak, from the peak intensity A_P.

2.8. Gas chromatography (GC)

GC analyses were performed on TRACE GC apparatus (ThermoQuest, Italy), equipped with a capillary column (Quadrex,

USA) with the following specifications: 5% phenyl methylpolysiloxane, 10 m length, I.D. 0.53 mm, 0.1 μm film thickness, a PTV injection was used at a split ratio of 1 : 10, inlet temperature was 80 °C, injection phase was 0.10 min, transfer phase of 5 min and a temperature of 350 °C (at a rate of 12 °C s^{-1}). The oven was programmed as follows: start at 120 °C, hold for 1 min, ramp 1: to 325 °C at 10 °C min^{-1}, ramp: 2 to 345 °C at 5 °C min^{-1}, hold for 5 min. The flame-ionization detector (FID) temperature was set to 350 °C. The carrier gas was helium, set in a constant pressure flow mode (60 kPa). The detector gases were hydrogen and air, with nitrogen as the make-up gas. All gases were of 99.999% purity.

An illustrative chromatogram obtained by the procedure described above, is presented in Fig. 2. The different peaks were identified using the standard substances described in Section 2.1. The fatty acids are observed to elute first, at retention times from 2 to 6 min. They are followed by the region of monoglycerides, which elute at 8.7, 8.9 and 9.1 min. Cholesterol elutes around 10.7 min, and the non-conjugated bile acids elute in the window 12–14 min. The diglycerides are detected in the range 15–18 min and the triglycerides are eluted after 22 min. Note that the oleic and linoleic acids, which represent ≈80% of the fatty acids in sunflower oil,[63] form a single peak with a regular shape.

The chromatograms were analyzed with the following integration parameters: peak width – 3 s, peak threshold – 3, minimum area – 5000, and skim ratio – 100. Manual integration was applied where needed. The obtained peak areas were corrected with response factors to account for the fact that different substances caused different detector responses. The following response factors were used to multiply the peak areas: 1.0 for fatty acids and monoglycerides, and 1.15 for cholesterol and diglycerides. These factors were determined by analyzing standard mixed solutions, containing fatty acids, mono- and diglycerides, and cholesterol of known concentrations. The TG concentration was not determined from the GC data, because of the bad baseline around the TG peak and irreproducible loss of material due to partial thermal decomposition.

After determining the quantities of all lipid components, we checked whether the molar balance of the fatty acid chains was satisfied, by comparing the moles of FFA, MG and DG from the GC, and the moles of TG from the TLC, on one side, with the total moles of TG introduced initially in the reaction mixture, on the other side. The molar ratio of measured *vs.* initial glycerides was close to 1 (between 0.8 and 1.2). The differences observed in some samples (unsatisfied mass balance) were most probably due to the limited accuracy of the TLC measurements. In these cases, the mass balance was finely tuned by multiplying all measured substances in the final reaction mixture by an appropriate correction factor to ensure a self-consistent mass balance.

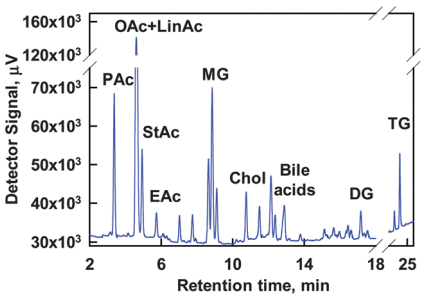

Fig. 2 Typical GC result, obtained with sunflower oil emulsion, subject to lipolysis and extraction with chloroform.

Summarizing, we determined by GC the amounts of MG, DG, cholesterol, and saturated and unsaturated FFA, whereas TLC was used to determine the amounts of TG.

2.9. Dynamic light-scattering (DLS)

To simplify the system composition, the solutions for these experiments were prepared by mixing all components, except for sunflower oil. In this way, no TG lipolysis occurred in these solutions. Note, however, that the solutions contained bile salts, phospholipids, free fatty acids and cholesterol introduced with the bile source (see Section 2.1). These solutions were centrifuged for 3 h at 3622*g* (4500 rpm) on a SIGMA 3-16PK centrifuge to obtain a clear aqueous phase (serum). Afterwards, one fraction of the serum was withdrawn by syringe and studied directly by DLS. Another fraction was first filtered through a 100 nm syringe filter and then subjected to DLS. The DLS was performed on a Malvern 4700C apparatus (Malvern Instruments, UK), equipped with a solid state Nd:YAG laser (λ_W = 532 nm). All described operations were performed at 37 °C.

2.10. Atomic absorption spectroscopy (AAS)

Calcium concentration in the aqueous phase was determined by AAS on an instrument Analyst 400 (PerkinElmer, USA) in an air/acetylene flame. The samples were prepared as follows: after filtration or centrifugation of the reaction mixture by the procedure described in Section 2.4, part of the sample was taken and diluted with solutions containing NaCl, KCl, NaN_3 and Na_2EDTA. We added Na_2EDTA to these solutions to prevent calcium precipitation, while NaN_3 was added as an antibacterial agent. The dilution was designed in such a way that all studied solutions had similar Ca^{2+} concentrations, falling around the middle of the calibration curves. The final concentrations of Na^+ and K^+ ions in the calibration solutions was equal to that in the studied solutions, because these elements interfere with calcium when measured by AAS.[64]

2.11. Degree of TG hydrolysis

TG transformations to DG and MG occurs *via* consecutive reactions.[65] Hence, we define three quantitative characteristics of TG transformation – overall degree of TG transformation, α; degree of TG transformation to DG, β, and degree of transformation to MG, γ. These three characteristics are related: $\alpha = \beta + \gamma$.

The overall degree of TG transformation is defined as:

$$\alpha = \frac{C_{TG}^{INI} - C_{TG}}{C_{TG}^{INI}} \quad (3)$$

here C_{TG}^{INI} is the initial molar concentration of TG (which is known), and C_{TG} is the molar concentration of the remaining non-hydrolyzed TG, as determined by TLC. The value of α accounts for the relative amount of TG that has been transformed into both MG and DG.

The degree of TG transformation to DG is defined as:

$$\beta = C_{DG}/C_{TG}^{INI} \quad (4)$$

here C_{DG} is the molar concentration of the formed and non-hydrolyzed DG. The value of β accounts for the amount of TG which is transformed into DG, without further transformation to MG.

The degree of TG transformation to MG is defined as:

$$\gamma = C_{MG}/C_{TG}^{INI} \quad (5)$$

here C_{MG} is the molar concentration of the formed MG, as determined by GC. The value of γ could be determined also by the relation:

$$\gamma = \frac{C_{FA}}{C_{TG}^{INI}} - \alpha \quad (6)$$

where C_{FA} is the concentration of the formed FFA.

In practice, we determined the value of α from the initial and the final TG concentrations, eqn (3), and the value of γ was determined from C_{MG}, using eqn (5). The value of β was determined by the relation $\beta = (\alpha - \gamma)$, because the concentration of FFA was determined with higher accuracy than the concentration of DG. The latter concentration was used only to check whether the overall mass balance of the glycerides was satisfied.

2.12. Transmission electron cryo-microscopy (cryo-TEM)

The cryo-samples were prepared using a CryoPlunge 3 unit (Gatan Instruments) employing a double blot technique. Briefly, 3 μL of the studied solution was pipetted onto a 15 s plasma etched, 400 mesh holey carbon grid (Agar Scientific), held in the plunge chamber at approx 90% humidity. The samples were blotted from both sides for 0.5, 0.8, or 1.0 s. The samples were then plunged into liquid ethane at a temperature of −170 °C. The grids were blotted to remove the excess ethane, then transferred under liquid nitrogen at −170 °C to a cryo-TEM specimen holder (Gatan 626). The samples were examined with a Jeol 2100 TEM, operated at 200 kV, and were imaged using a Gatan Ultrascan 4000 camera and DigitalMicrograph software (Gatan).

3. Results and discussion

3.1. Comparison of the *in vitro* procedure and the *in vivo* conditions

The experimental conditions in our *in vitro* procedure are formulated to mimic closely the electrolyte concentrations in the stomach, duodenum and jejunum, as reported in literature,[66–79] see Table 1. In our first series of experiments, we measured pH of the reaction mixture as a function of time and its evolution was found to be rather reproducible in the course of the experiment, ±0.15 pH units. As seen from Fig. 3, the pH-profile of our *in vitro* procedure closely resembles the pH profile determined in the *in vivo* experiments. The concentration of the pancreatic enzymes is chosen to be in excess with respect to the enzyme substrates, as it is *in vivo*. Thus we can conclude from Table 1 and Fig. 3 that the pH profile, and the electrolyte, bile and enzyme concentrations in our *in vitro* model resemble closely those found *in vivo*.

3.2. Effect of bicarbonate on the TG hydrolysis, at different Ca^{2+} concentrations

To check whether the presence of bicarbonate in the reaction mixture has any effect on the lipolysis reaction, we performed comparative experiments using two procedures – with bicarbonate (as described in Section 2.3) and without bicarbonate (pH-dynamic, Section 2.4). Note that the pH-profiles in these two procedures are very similar.

The results for the degree of TG hydrolysis, α, obtained by these two procedures, are compared in Fig. 4. For all Ca^{2+} concentrations studied, the TG hydrolysis in the presence of bicarbonate is found to be somewhat higher than that measured without carbonate. The other important difference was the overall trend of the dependence of α *vs.* Ca^{2+} concentration, C_{Ca}. This dependence passes through a minimum for the solutions with bicarbonate, whereas in the absence of bicarbonate α is almost constant, up to 6 mM Ca^{2+}, and decreases significantly at 11 mM Ca^{2+}. Therefore, we can conclude that the bicarbonate has a noticeable impact on the dependence of α on Ca^{2+} concentration.

Let us discuss the dependence of α on C_{Ca} for the experiments performed in the presence of bicarbonate. The first important comment is that the degree of TG hydrolysis does not achieve 100%, even after 4.5 h of reaction time. The highest degree, observed at the lowest Ca^{2+} concentration, is ≈80%. This concentration, C_{Ca} = 1 mM, corresponds to the physiological conditions and the measured value of α is in very good agreement with the *in vivo* results, reported earlier for similar reaction times – for example, Armand *et al.*[81] found that TG lipolysis in the duodenum is ≈73% after 4 h. Therefore, the used experimental procedure gives results which are comparable to those found in the *in vivo* experiments. The increase of C_{Ca} above the physiological value of 1 mM leads to lower TG hydrolysis, which passes through a shallow minimum at 3.5 mM Ca^{2+} in the presence of bicarbonate ($\alpha \approx 65\%$). However, this effect of C_{Ca} seems to be not very significant and probably has no important physiological consequences, unless combined with other effects.

The observed higher values of α in the presence of bicarbonate can be explained by the binding of Ca^{2+} to the HCO_3^- ions, which results in decreased concentration of soluble Ca^{2+} ions in the solution. Lower concentrations of soluble Ca^{2+} should lead

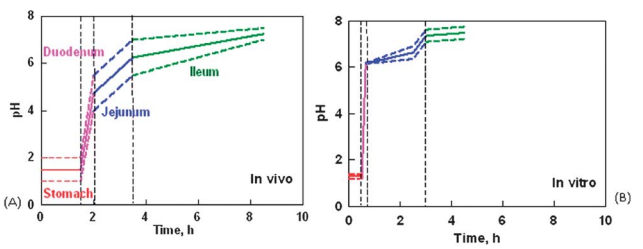

Fig. 3 pH in the upper gastro-intestinal tract (GIT), as a function of reaction time (A) *in vivo*, adapted from Daugherty and Mrsny[80] and (B) in our *in vitro* model with carbonate. The solid lines indicate the mean values from 8 independent measurements, while the dashed lines indicate the minimal and maximal values in these measurements. The different parts of the GIT are separated by vertical dashed lines and are color coded as follows: stomach – red; duodenum – pink; jejunum – blue; ileum – green.

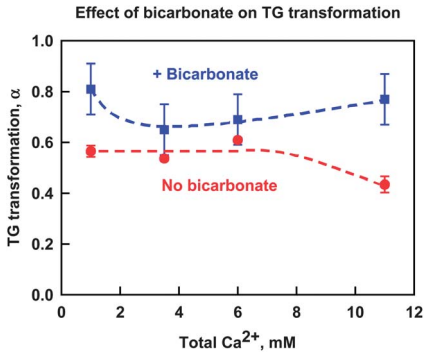

Fig. 4 Degree of TG transformation, α, as a function of Ca^{2+} concentration in the aqueous phase, in the presence of bicarbonate (blue squares) and in the absence of bicarbonate (red circles). The experimental data in the presence of bicarbonate are the average of 4 independent series of experiments, while those without bicarbonate are from 2 independent series of experiments. The lines are eye-guides.

to less precipitates of Ca^{2+}-soaps on the drop surface. These precipitates are known to impede TG lipolysis due to the reduced contact area of the triglycerides in the oil drops with the pancreatic lipase.[82,83]

Let us compare now our results for the effect of Ca^{2+} ions on the degree of TG lipolysis with those of other authors. In most *in vitro* studies, the authors reported significant increases of TG hydrolysis with the increase of Ca^{2+} concentration[7,11,42] – an effect that has not been observed in our experiments. When analyzing the possible reasons for this apparent discrepancy, we noticed several important differences in the experimental procedures used in these studies:[7,11,42]

(1) In our experiments (and *in vivo*) the bile salts have molar concentrations which are in excess of that of the TG and the lipolysis products – see the table with the composition of the reaction mixture, shown in Fig. 1. In contrast, in all articles where a strong effect of Ca^{2+} on lipolysis was reported[7,11,42] the TG and lipolysis products were in excess with respect to the bile salts. Some authors have already suggested[7] that the main reason for the observed significant effect of Ca^{2+} could be the relatively low ratio of bile salts/lipolysis products, used in the respective studies;

(2) The pH in the other studies was fixed, whereas in our experiments pH increased during the experiment, following the pH profile in the human GIT. This pH evolution should lead to an increase of the solubility of the reaction products along the experiment, especially at low Ca^{2+} concentrations, at which the other authors reported rather low degrees of TG hydrolysis (smaller than 30%);

(3) The time scale in the previous experiment was between 20 and 40 min, whereas our experiments were much longer (4 h) to mimic better the intestinal conditions.

(4) The effect of Ca^{2+} ions could depend on the type of studied triglycerides. The results reported in the current study are obtained with sunflower oil only. This oil is characterized with a rather low content of saturated fatty acid chains in its molecules (around 10% of palmitic and stearic acids, the rest are mainly linoleic and oleic acids). Our preliminary experiments demonstrated much larger effects of calcium for triglycerides containing a higher fraction of saturated fatty chains, such as lard, palm oil, butter fat, and cocoa butter (these results will be a subject of a subsequent paper).

Therefore, we cannot expect direct agreement between our results and those reported by other authors for the effect of Ca^{2+} on α, while we consider our *in vitro* conditions to represent better the *in vivo* conditions in the human GIT.

The main conclusion from all these experiments is that the presence of bicarbonate in the solution affects the degree of TG hydrolysis, especially at high Ca^{2+} concentrations, which is most probably due to binding (complex formation) of Ca^{2+} cations to the bicarbonate anions.

3.3. Effect of the pH-profile on TG hydrolysis, at different Ca^{2+} concentrations

As shown in Fig. 3A, the pH profile in the human tract varies in a certain range from individual to individual, and it depends on the type and amount of food consumed. In the previous subsection we presented results about the effect of Ca^{2+} on the degree of TG hydrolysis, in experiments where the pH profile reached 7.5 after 4 h – this profile corresponds to the upper boundary observed in the clinical studies.

In the current section we present results about the effect of Ca^{2+} concentration on TG lipolysis using a modified procedure, in which the pH profile corresponds to the lower boundary found *in vivo* (pH reached 6.8 after 4 h). In this series of experiments we stirred the samples with bicarbonate for 4 h in a closed vessel, as explained in Section 2.2.

The results for the TG hydrolysis, obtained by these two procedures (higher and lower final pH), are compared in Fig. 5. One sees that the values of α show very similar trends for both pH profiles, when plotted as functions of C_{Ca}. The main difference is that the degree of TG hydrolysis is somewhat higher for the higher pH. This effect could be explained by the better solubility of the reaction products and/or by higher enzyme activity, at the higher pH. Note also that at the physiological Ca^{2+} concentration of 1 mM, the value of α in both procedures is very similar – this means that the pH variation in the physiological range does not affect significantly the degree of TG lipolysis. However, in the range between 3 and 6 mM Ca^{2+}, a noticeably lower degree of TG hydrolysis is observed at the lower pH.

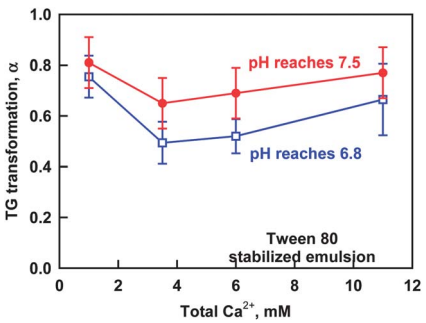

Fig. 5 Degree of TG transformation, α, as a function of Ca^{2+} concentration for solutions where the pH reaches 7.5 (red circles) or 6.8 (blue squares) at the end of the lipolysis reaction. All experimental points are the average of at least three independent experiments.

From now on, we present experimental results obtained with the procedure leading to a final pH of ≈ 6.8, unless otherwise specified. This procedure was chosen for most experiments, because the observed effects were more pronounced, as compared to the procedure at which the final pH was ≈ 7.5.

Along with the total degree of TG hydrolysis, α, we measured the TG hydrolysis to MG and DG, represented by the values of γ and β (see eqn (3)–(5)). From Fig. S2†, it can be seen that the main fraction of TG is transformed into MGs, at all Ca^{2+} concentrations studied. Only about 10% of the TG is transformed into DG after 4 h of reaction time.

Thus we conclude from these experiments that: (1) TG hydrolysis passes through a shallow minimum at 3 mM Ca^{2+}; (2) the increase of pH increases the TG hydrolysis for Ca^{2+} concentrations ≥3.5 mM and does not significantly affect TG hydrolysis at 1 mM Ca^{2+}; (3) TG is hydrolyzed preferentially to MG when $\alpha > 0.5$, regardless of Ca^{2+} concentration.

3.4. Effect of Ca^{2+} on the composition of the aqueous phases

In this section we present results about the concentrations of the lipolysis products (free fatty acids, monoglycerides, diglycerides) and cholesterol in the aqueous phase. All experiments were performed using the procedure described in Section 2.3, with the pH-profile reaching a final pH of ≈ 6.8.

3.4.1. Illustrative results for the effect of the phase separation procedure on the solubilization of reaction products. The studied systems are heterogeneous – typically, they contain an oily phase, solid phases (precipitates), and an aqueous phase. In the literature, ultracentrifugation,[2,3,12,14] filtration[84] or dialysis[18] are used for phase separation in such systems. Each of these methods has certain advantages and disadvantages. Ultracentrifugation is relatively easy but it disturbs the phase equilibrium and could cause changes in the material distribution between the various phases. Filtration at low pressure is a mild method for phase separation, but here the question being what is the relevant filter pore size. Dialysis is a very slow process and again questions appear about the appropriate membrane cut-off and the possible disturbance of the phase equilibrium. Therefore, none of these methods are perfect.

We applied two procedures for the separation and subsequent analysis of the aqueous phase – centrifugation and filtration, see Section 2.5. The aqueous phase passing through the filters is called "a permeate" in the following discussion. The filter pore size of 200 nm was chosen because, according to literature,[85,86] entities smaller than 200 nm easily pass through the mucus layer. However, it is known that transport through the mucus membrane depends significantly on the adhesive properties of the particles as well.[87,88] Therefore, this filtration procedure gives information about the size of the aggregates, but no direct conclusions about the bioavailability of the components could be made.

The centrifugation was performed for 1 hour at 3620*g* (4500 rpm) at 37 °C and it allowed us to characterise the bigger aggregates which were present in some of the samples. The clear aqueous phase, obtained after centrifugation, will be called hereafter "a serum". The lipophilic components in the serum and permeate were extracted as described in Section 2.6 and analyzed by TLC and GC.

Illustrative results from the TLC analysis of the serum and permeate are shown in Fig. S3.† The results obtained with the extract from the whole sample (non-filtered and non-centrifuged) are also shown in Fig. S3† for comparison. It can be seen that both the serum and the permeate do not contain any TG, whereas the whole sample contains a significant amount of non-hydrolyzed TG (see the first lane in Fig. S3†). A noticeable difference between the serum and permeate is observed with respect to the concentrations of FFA, DG, MG and cholesterol – *cf.* the second and fourth lanes in Fig. S3.† The concentrations of all these substances are lower in the permeate obtained after filtration through the 200 nm filter, as compared to the serum obtained after centrifugation.

For quantitative analysis of these substances we used GC. As an illustration, we show in Fig. 6 the regions in the GC chromatograms, corresponding to the fatty acids and cholesterol. It can be seen that the peaks for palmitic, stearic, and oleic + linoleic acids correspond to much higher concentrations in the serum, as compared to the permeate. A significant difference is also observed for the peaks of cholesterol in the serum and the permeate.

To analyze the reasons for the different compositions of the serum and the permeate, we measured the concentration of Ca^{2+} in these phases by AAS, and the size and type of the molecular aggregates by DLS and cryo-TEM – these results are described in the following Section 3.4.2. The entire set of data for the compositions of the serum and permeate, at different Ca^{2+} concentrations, is presented and discussed in Section 3.4.3.

3.4.2. Determination of soluble Ca^{2+} concentration and characterization of the molecular aggregates. The concentration of soluble Ca^{2+} in the aqueous phase (serum or permeate) was determined by AAS and the results are presented in Fig. 7. It can be seen that most of the calcium is in the soluble form at $C_{Ca} \leq 6$ mM, whereas the calcium measured in the permeate is significantly less than that in the serum at 11 mM Ca^{2+}. This difference could only be explained by assuming that relatively large Ca^{2+}-binding colloid aggregates are formed at high Ca^{2+} concentration (*e.g.*, vesicles or planar aggregates) which cannot pass through the 200 nm filter, while still being sufficiently small enough to remain dispersed after centrifugation.

To analyze the contents of the serum and permeate with respect to the aggregate size, we used dynamic light-scattering (DLS). These experiments were performed without adding triglyceride oil to the solutions, in order to simplify the data

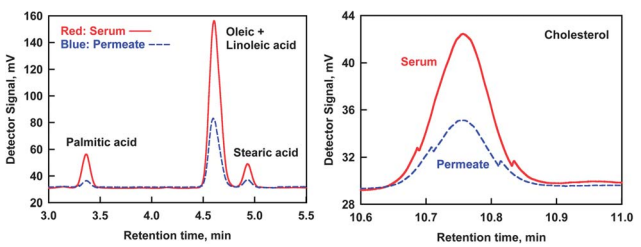

Fig. 6 GC results for the serum obtained after centrifugation (red solid curves) and the permeate obtained after filtration (blue dashed curves) of the reaction mixture, after extraction with chloroform. The lipolysis is performed in presence of 11 mM $CaCl_2$.

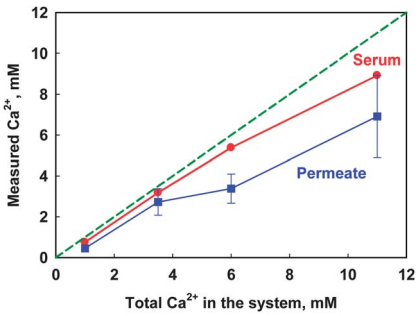

Fig. 7 Calcium measured by AAS in the serum after centrifugation (red circles) and in the permeate after filtration (blue squares) *vs.* the total calcium present in the system. The dashed line indicates the concentration that would be measured if all calcium was dissolved in the aqueous phase and/or bound to the small bile micelles. The difference between the dashed line and curve for the serum shows the amount of the precipitated calcium, whereas the difference between the curve for the serum and the curve for the permeate shows the calcium bound to the large molecular aggregates with size >200 nm.

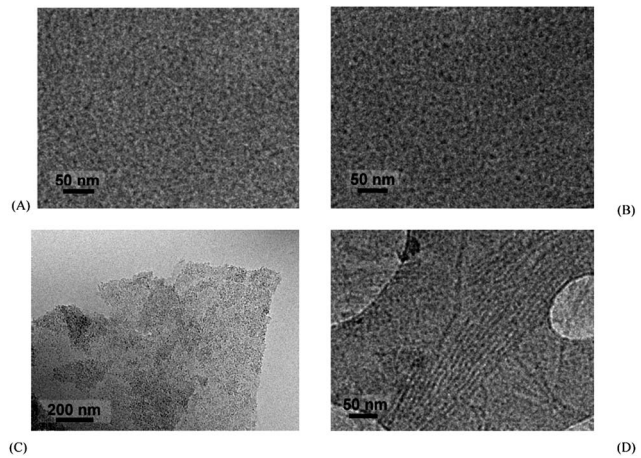

Fig. 8 Cryo-TEM micrographs of the aqueous phase after lipolysis, in the presence of (A and B) 1 mM Ca^{2+}, (C and D) 11 mM Ca^{2+}, (A and C) serum after centrifugation, and (B and D) permeate after filtration. Only small dietary micelles are seen in (A) and (B), whereas both small and large micelles are seen in (C) and (D). The lipolysis experiments are described in Section 2.3, the aqueous phase was separated as described in Section 2.5, and the cryo-TEM procedure is described in Section 2.13.

interpretation – all the other components were mixed as usual. The results are presented in Fig. S4.† It can be seen that the mean particle diameter is typically around 4 nm in the permeate after filtration, which is in good agreement with the size of the small bile micelles reported in the literature.[5,89,90] The size of these micelles remains constant with the increase of calcium concentration up to 6 mM. At the highest concentration of 11 mM Ca^{2+}, however, bigger aggregates with a diameter of around 30 nm were registered in the permeate. On the other hand, the aggregates in the serum after centrifugation had a diameter of 30 nm, even at the lowest Ca^{2+} concentration, and this diameter increased up to $\approx$300 nm at the higher Ca^{2+} concentrations.

To clarify what is the type of large aggregates detected by DLS, we used cryo-TEM for investigation of the systems after TG lipolysis, at 1 mM and 11 mM Ca^{2+}. These experiments are performed after digestion process (in presence of FFA). Representative images of vitrified samples of the serum and the permeate are shown in Fig. 8. Note that for all these systems, the concentration of the lipolysis products is similar, as the degree of TG hydrolysis is $\alpha \approx 0.8$. At the low Ca^{2+} concentration of 1 mM, only small micelles are seen in both the permeate and the serum. In contrast, at 11 mM Ca^{2+} we observe large planar aggregates in the serum, and worm-like aggregates in the permeate. Single small micelles can be also seen in these samples. Similar in structure and size aggregates were observed in a model lipolysis system by other authors.[90,91]

The obtained results allow us to conclude that: (1) only a small fraction of Ca^{2+} precipitates in these systems, (2) at high concentrations, calcium induces formation of calcium-binding large aggregates, which are retained upon filtration with a 200 nm filter. The formation of these large aggregates explains the different concentrations of Ca^{2+} in the serum and in the permeate – the large aggregates bind very efficiently the calcium ions.

3.4.3. Effect of Ca^{2+} on the quantity of soluble reaction products and cholesterol

Free fatty acids (FFA). The results for the concentration of free fatty acids (FFA) measured in the whole sample (before phase separation), and in the serum and permeate, are compared in Fig. 9A. It can be seen that the total concentration of solubilized FFA has a shallow minimum at 3.5 mM Ca^{2+}, which is in accordance with the observed minimum in the degree of TG transformation.

The dependences of FFA on C_{Ca}, as measured in the permeate and in the serum, are different. In the permeate, the concentration of FFA decreases steadily with the increase of Ca^{2+} concentration, while in the serum this concentration increases significantly at 6 and 11 mM Ca^{2+} (and almost reaches the value of the total FFA concentration).

At the lowest Ca^{2+} concentration studied, 1 mM, the concentrations of FFA in the serum and in the permeate coincide, while they both differ by $\approx$3 mM (which is $\approx$30% of all fatty acids in the system) from the total concentration in the whole sample, see Fig. 9A. This means that $\approx$30% of the total FFA is not in the aqueous phase at 1 mM Ca^{2+}. These "missing" FFA could be either in the oily drops, together with the non-hydrolyzed TG and DG, or in the sediment where FFA can co-precipitate with Ca^{2+}. For brevity, hereafter we use the term "water-insoluble" FFA for those fatty acids which are missing from the aqueous phase, though this term is not precise. From the measured soluble Ca^{2+} in the samples, see Fig. 7, we know that the precipitated Ca^{2+} is only $\approx$0.3 mM. Assuming that the precipitated calcium binds two FFA per Ca^{2+} ion, we estimate that the maximum amount of co-precipitated FFA should be $\approx$0.6 mM. Therefore, we estimate that the main fraction of the FFA (around 2.4 mM), which is absent from the aqueous phase at 1 mM Ca^{2+}, is trapped in the oily drops.

At 3.5 mM Ca^{2+} we measured different FFA concentrations in the serum and in the permeate, which means that some fraction of FFA (around 1 mM) are solubilised in the large aggregates with sizes larger than 200 nm. The water-insoluble fraction of the FFA is $\approx$2.2 mM (this is the difference between FFA in the whole sample and in the serum) and it is very similar to that

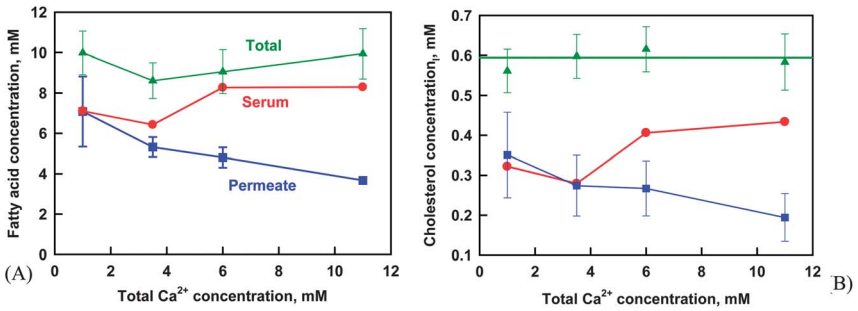

Fig. 9 Concentration of (A) solubilized free fatty acids and (B) solubilized cholesterol, as a function of the total Ca^{2+} concentration, in the whole sample (green triangles), in the serum after centrifugation (red circles), and in the permeate after filtration (blue squares). All experimental points are average of at least three independent experiments.

measured at 1 mM Ca^{2+}. Note, that while the total Ca^{2+} was increased from 1 to 3.5 mM, the precipitated Ca^{2+} remained at $\approx$0.3 mM, which means that only around 0.6 mM out of the 2.2 mM FFA could be co-precipitated with Ca^{2+} (*viz.* 30% of all FFA). Thus we again conclude that the main fraction of the water-insoluble FFA is trapped in the oily drops.

At 6.5 mM Ca^{2+}, the FFA concentration is 8.3 mM in the serum, whereas it is only 4.8 mM in the permeate. This significant difference indicates that 3.5 mM FFA are trapped in molecular aggregates with sizes larger than 200 nm. The water-insoluble fraction of FFA decreases from 2.4 mM down to 0.7 mM, while the quantity of the oily drops (containing TG and DG) is almost the same for 1 and 6 mM Ca^{2+}. This result indicates that the large molecular aggregates are able to extract efficiently the FFA from the oily drops.

Further increases of Ca^{2+} concentration decreases significantly the amount of FFA, which are solubilized in the micelles (in the permeate), down to 3.7 mM. The concentration of FFA bound to large aggregates increases to 4.6 mM, while the water-insoluble fraction of FFA is $\approx$1.6 mM.

From all these data we can conclude that the increase of Ca^{2+} concentration leads to formation of large molecular aggregates, which are able to solubilize very efficiently the FFA. The main fraction of FFA is incorporated in the small micelles at the lowest Ca^{2+} concentration, whereas it is in the large aggregates at the highest Ca^{2+} concentration. The decrease of the FFA solubilised in the small micelles, observed with the increases of Ca^{2+} concentration, is in qualitative agreement with the clinical studies showing that the excretion of FFA increases at high Ca intake.[33,34]

Saturated free fatty acids (saturated FFA). Along with the total concentration of FFA in the aqueous phase, another interesting quantity is the concentration of saturated FFA in the micelles, large aggregates, and in water-insoluble form (precipitates or oily drops).

The obtained results for the concentrations of the saturated FFA in the whole sample, the serum and the permeate are compared in Fig. S5.† One sees that the total concentration of saturated FFA is almost constant $\approx$3.2 mM and does not depend significantly on Ca^{2+} concentration. This is rather interesting result, as far as the total concentration of FFA (including both saturated and unsaturated) passes through a minimum at 3.5 mM Ca^{2+}, see Fig. 9A. This result suggests that the saturated FFA might be digested preferentially by the enzyme.

At the lowest Ca^{2+} concentration, the saturated FFA in the permeate and in the serum are similar, because the small micelles are the dominant molecular aggregates under these conditions.

The amount of saturated FFA in the permeate after filtration decreases from 1.35 mM to 0.8 mM with the increase of Ca^{2+} concentration up to 6 mM, and remains constant with further increases to 11 mM. Therefore only 25% of the total saturated FFA are solubilised in the small micelles at $C_{Ca} \geq 6$ mM. The concentration of saturated FFA in the serum increases with the increase of C_{Ca} and one can estimate from these data that $\approx$50% of the total concentration of saturated FFA is included in large aggregates at 6 and 11 mM Ca^{2+}.

In Fig. S6† we plot the ratio of the saturated FFA to the total concentration of (saturated + unsaturated) FFA, as a function of Ca^{2+} concentration. It can be seen that the fraction of saturated FFA remains constant in the permeate (*viz.* in the small micelles), while it increases in the serum (*i.e.*, in the large molecular aggregates). Thus, the large aggregates formed at high Ca^{2+} concentrations contain more saturated FFA, while the calcium does not affect the content of saturated FFA in the micelles.

Concluding, the increase of Ca^{2+} concentration decreases the concentration of saturated FFA in the micelles, but increases it significantly in the large aggregates.

Cholesterol. The results for the effect of Ca^{2+} on the concentration of cholesterol in the permeate, the serum and the whole sample are compared in Fig. 9B. The cholesterol in our experiments is coming from the bile source only and, as the bile salts concentration is kept constant in these experiments, so should the total cholesterol. Indeed, the concentration of cholesterol was determined to be the same, $\approx$0.6 mM, for all non-filtered and non-centrifuged samples. This is a very good indication of the reproducibility and self-consistency of the used analytical procedures.

We found that the cholesterol concentrations in the serum and in the permeate show the same trends as the concentrations of FFA: the cholesterol decreases with the increase of Ca^{2+} concentration in the permeate, while it increases in the serum at Ca^{2+} concentrations above 6 mM. These results indicate that, similar to the FFA, the cholesterol is solubilized preferentially in

the large aggregates, as compared to the small micelles. The higher concentration of large aggregates, formed at high Ca^{2+} concentrations, leads to higher cholesterol concentrations in the serum, compared to its concentration in the permeate. In the same line of thought, the difference between the serum and the permeate increases with the increase of Ca^{2+} concentration, due to the formation of more large aggregates which solubilise better the cholesterol.

The experiments showed that, even at the lowest Ca^{2+} concentration, only 60% of the total cholesterol is in soluble form, which is in good agreement with the reported values from *in vivo* experiments.[92,93] Therefore, about 40% of the cholesterol is trapped in the precipitates and/or is dissolved in the oily TG–DG droplets under these conditions.

To check for a possible correlation between the amounts of solubilised FFA and cholesterol, we plotted the concentration of cholesterol *vs.* the concentration of FFA for both aqueous phases studied – after filtration and after centrifugation. We see in Fig. 10 a very good correlation between the concentrations of cholesterol and FFA, which means that these two substances co-solubilize in the micelles and in the large aggregates. From these data, we can calculate that around 22 molecules of FFA co-solubilize with 1 cholesterol molecule at the used bile salts concentration of 15 mM and cholesterol concentration of 0.6 mM.

Monoglycerides. Finally, we present results for the concentration of MG in the serum and in the permeate, see Fig. S7.† The total concentration of MG correlates with the degree of TG transformation and has a shallow minimum at 3.5 mM Ca^{2+}, as expected. On the other hand, most of the MG passes through the filter in the permeate, which means that the main fraction of MG is solubilized inside the small micelles. Only at high Ca^{2+} concentrations does a fraction of the MG solubilize in the large aggregates as well.

We can conclude from all these experiments that the cholesterol and free fatty acids solubilise preferentially in the large aggregates at high Ca^{2+} concentrations, whereas MGs are solubilised preferentially within the small micelles.

Finally, we note that the obtained results for the distribution of reaction products and cholesterol at low Ca^{2+} concentrations are in a good agreement with the results obtained by Kossena *et al.*,[94] where (by using model mixtures) these authors showed that MG and FFA are predominantly solubilised in the small micelles, as compared to the large aggregates.

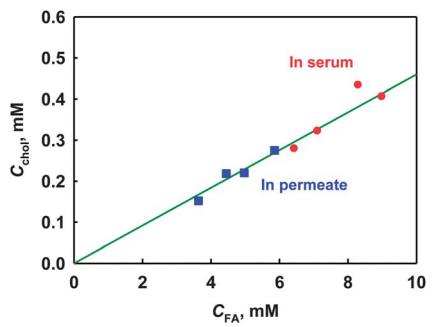

Fig. 10 Concentration of the solubilized cholesterol *vs.* the concentration of the solubilized FFAS in the permeate after filtration (squares), and in the serum after centrifugation (circles).

4. Conclusions

We have studied triglyceride lipolysis by pancreatic lipase and the phase distribution of the reaction products and cholesterol, at conditions resembling those in the small intestine. To match these conditions, we developed an *in vitro* lipolysis model which uses bicarbonate to realize the pH-profile seen *in vivo*. The model is relatively simple, does not require special or expensive equipment, and allows the study of several samples per day. Filtration and centrifugation were used to separate the aqueous phase from the heterogeneous reaction mixture, at the end of the lipolysis reaction. These procedures allowed us to study the degree of TG lipolysis and the solubilization of the lipolysis products and the cholesterol in the aqueous phase. The effects of Ca^{2+}, pH profile, and the presence of carbonate were particularly addressed.

The main conclusions with respect to the degree of TG hydrolysis are as follows:

- The degree of TG hydrolysis passes through a shallow minimum at 3.5 mM Ca^{2+}.
- The presence of bicarbonate in the reaction mixture leads to a higher degree of hydrolysis, especially at high calcium concentrations.
- The comparison of the degree of TG hydrolysis at two pH profiles, reaching pH = 6.8 and 7.5, respectively, showed that the degree of TG lipolysis increases with pH.
- The TG is hydrolyzed preferentially to MG, where only a small fraction remains as DG.

With respect to the phase distribution of the lipophilic substances, the main conclusions are as follows:

- The cholesterol solubilized in the aqueous phase increases linearly with the concentration of the solubilised FFA, with a slope of 46 mg g^{-1} cholesterol–FFA. Thus, around 22 molecules of FFA co-solubilize with 1 molecule of cholesterol in the bile aggregates under the conditions studied (fixed concentrations of cholesterol and bile salts in the reaction mixture – 0.6 mM and 15 mM, respectively).
- The increase of Ca^{2+} concentration above 3 mM leads to the formation of large aggregates which cannot pass through a nylon filter with a pore size of 200 nm.
- The cholesterol and saturated fatty acids are solubilized preferentially in the large aggregates (formed at high Ca^{2+} concentrations), whereas the monoglycerides are preferentially solubilized in the small bile micelles.

Let us note at the end that the described *in vitro* model is appropriate for studying other phenomena, such as the phase distribution and bioavailability of lipophilic drugs, effect of food ingredients and supplements on the shape and size of the bile salt aggregates, precipitation of bile salts and fatty acids under physiologically relevant conditions, and many others. This makes it a versatile tool for studying the lipid-related phenomena occurring in the GIT.

Acknowledgements

The authors are grateful to Dr S. Furzeland and Dr D. Atkins for performing the cryo-TEM observations, Mr G. Sasano for

sharing his GC experience in lipid analysis, Dr P. Rayment and Dr S. Pregent for the useful discussions (all from Unilever R&D, Colworth, UK), Dr Y. Atanasov for his involvement in the initial development of the *in vitro* model, Ms Z. Mitrinova for her help in performing some of the *in vitro* experiments and Dr I. Karadjova for performing the AAS measurements (all from Sofia University). The stimulating useful discussions with Dr G. Duchateau and Dr E. Pelan on the *in vivo* conditions, are gratefully acknowledged (both from Unilever R&D, Vlaardingen, The Netherlands). The authors are grateful to Unilever R&D and FP7 Project Beyond Everest for the support.

References

1 P. Tso and K. Crissinger, Overview of Digestion and Absorption, in *Biochemical and Physiological Aspects of Human Nutrition*, ed. M. H. Stipanuk, WB Saunders Company, Philadelphia, 2000, pp. 75–90.
2 A. F. Hofmann and B. Borgström, Physico-chemical state of lipids in intestinal content during their digestion and absorption, *Fed. Proc.*, 1962, **21**, 43–50.
3 A. F. Hofmann and B. Borgström, The intraluminal phase of fat digestion in man: the lipid content of the micellar and oil phases of intestinal content obtained during fat digestion and absorption, *J. Clin. Invest.*, 1964, **43**, 247–257.
4 J. S. Patton and M. C. Carey, Watching fat digestion, *Science*, 1979, **204**, 145–148.
5 J. E. Staggers, O. Hernell, R. J. Stafford and M. C. Carey, Physical-chemical behavior of dietary and biliary lipids during intestinal digestion and absorption. 1. Phase behavior and aggregation states of model lipid systems patterned after aqueous duodenal contents of healthy adult human beings, *Biochemistry*, 1990, **29**(8), 2028–2040.
6 O. Hernell, J. E. Staggers and M. C. Carey, Physical-chemical behavior of dietary and biliary lipids during intestinal digestion and absorption. 2. Phase analysis and aggregation states of luminal lipids during duodenal fat digestion in healthy adult human beings, *Biochemistry*, 1990, **29**(8), 2041–2056.
7 K. J. MacGregor, J. K. Embleton, J. E. Lacy, E. A. Perry, L. J. Solomon, H. Seager and C. W. Pouton, Influence of lipolysis on drug absorption from the gastro-intestinal tract, *Adv. Drug Delivery Rev.*, 1997, **25**(1), 33–46.
8 D. G. Fatouros and A. Mullertz, *In vitro* lipid digestion models in design of drug delivery systems for enhancing oral bioavailability, *Expert Opin. Drug Metab. Toxicol.*, 2008, **4**(1), 65.
9 J. Ø. Christensen, K. Schultz, B. Mollgaard, H. G. Kristensen and A. Mullertz, Solubilisation of poorly water-soluble drugs during *in vitro* lipolysis of medium- and long-chain triacylglycerols, *Eur. J. Pharm. Sci.*, 2004, **23**(3), 287–296.
10 H. Mu and C.-E. Høy, The digestion of dietary triacylglycerols, *Prog. Lipid Res.*, 2004, **43**(2), 105–133.
11 N. H. Zangenberg, A. Mullertz, H. G. Kristensen and L. Hovgaard, A dynamic *in vitro* lipolysis model I: controlling the rate of lipolysis by continuous addition of calcium, *Eur. J. Pharm. Sci.*, 2001, **14**, 115.
12 N. H. Zangenberg, A. Mullertz, H. G. Kristensen and L. Hovgaard, A dynamic *in vitro* lipolysis model II: evaluation of the model, *Eur. J. Pharm. Sci.*, 2001, **14**, 237.
13 C. J. H. Porter and W. N. Charman, *In vitro* assessment of oral lipid based formulations, *Adv. Drug Delivery Rev.*, 2001, **50**, S127–S14746.
14 L. Sek, C. J. H. Porter, A. M. Kaukonen and W. N. Charman, Evaluation of the *in vitro* digestion profiles of long and medium chain glycerides and the phase behaviour of their lipolytic products, *J. Pharm. Pharmacol.*, 2002, **54**, 29.
15 C. J. H. Porter, N. L. Trevaskis and W. N. Charman, Lipids and lipid-based formulations: optimizing the oral delivery of lipophilic drugs, *Nat. Rev. Drug Discovery*, 2007, **6**, 231–248.
16 A. Dahan and A. Hoffman, The effect of different lipid based formulations on the oral absorption of lipophilic drugs: the ability of *in vitro* lipolysis and consecutive *ex vivo* intestinal permeability data to predict *in vivo* bioavailability in rats, *Eur. J. Pharm. Biopharm.*, 2007, **67**, 96.
17 R. Havenaar and M. Minekus, *In vitro* model of an *in vivo* digestive tract, *European Pat.* PCT/NL93/00225, 1994.
18 M. Minekus, M. Smeets-Peeters, A. Bernalier, S. Marol-Bonnin, R. Havenaar, P. Marteau, M. Alric, G. Fonty and J. H. H. Huis In't Veld, A computer-controlled system to simulate conditions of the large intestine with peristaltic mixing, water absorption and absorption of fermentation products, *Appl. Microbiol. Biotechnol.*, 1999, **53**, 108.
19 R. Verger and G. H. De-Haas, Enzyme reactions in a membrane model. 1. A new technique tostudy enzyme reactions in monolayers, *Chem. Phys. Lipids*, 1973, **10**, 127.
20 I. Panaiotov and R. Verger, Enzymatic Reactions at Interfaces: Interfacial and Temporal Organization of Enzymatic Lipolysis, in *Physical Chemistry of Biological Interfaces*, ed. I. Norde, Marcel Dekker, New York, 2000, ch. 11, pp. 359–400.
21 Y. Gargouri, R. Julien, A. G. Bois, R. Verger and L. Sarda, Studies on the detergent inhibition of pancreatic lipase activity, *J. Lipid Res.*, 1983, **24**(10), 1336–1342.
22 T. Tsujita, Inhibiting lipid absorption using basic biopolymers, *Future Lipidol.*, 2007, **2**(5), 547–555.
23 P. J. Wilde and B. S. Chu, Interfacial & colloidal aspects of lipid digestion, *Adv. Colloid Interface Sci.*, 2011, **165**(1), 14–22.
24 P. Reis, K. Holmberg, H. Watzke, M. E. Leser and R. Miller, Lipases at interfaces: a review, *Adv. Colloid Interface Sci.*, 2009, **147–148**, 237–250.
25 B.-S. Chu, G. T. Rich, M. J. Ridout, R. M. Faulks, M. S. J. Wickham and P. J. Wilde, Modulating pancreatic lipase activity with galactolipids: effects of emulsion interfacial composition, *Langmuir*, 2009, **25**(16), 9352–9360.
26 B.-S. Chu, A. P. Gunning, G. T. Rich, M. J. Ridout, R. M. Faulks, M. S. J. Wickham, V. J. Morris and P. J. Wilde, Adsorption of bile salts and pancreatic colipase and lipase onto digalactosyldiacylglycerol and dipalmitoylphosphatidylcholine monolayers, *Langmuir*, 2010, **26**(12), 9782–9793.
27 Y. Pafumi, D. Lairon, P. L. de la Porte, C. Juhel, J. Storch, M. Hamosh and M. Armand, Mechanisms of inhibition of triacylglycerol hydrolysis by human gastric lipase, *J. Biol. Chem.*, 2002, **277**(31), 28070–28079.
28 D. J. McClements, E. A. Decker and Y. Park, Controlling lipid bioavailability through physicochemical and structural approaches, *Crit. Rev. Food Sci. Nutr.*, 2009, **49**(1), 48–67.
29 S. J. Hur, E. A. Decker and D. J. McClements, Influence of initial emulsifier type on microstructural changes occurring in emulsified lipids during *in vitro* digestion, *Food Chem.*, 2009, **114**(1), 253–262.
30 D. J. McClements and Y. Li, Review of *in vitro* digestion models for rapid screening of emulsion-based systems, *Food Funct.*, 2010, **1**, 32–59.
31 A. N. Payne, A. Zihler, C. Chassard and C. Lacroix, Advances and perspectives in *in vitro* human gut fermentation modelling, *Trends Biotechnol.*, 2012, **30**(1), 17–25.
32 K. C. Maki, D. N. Butteiger, T. M. Rains, A. Lawless, M. S. Reeves, C. Schasteen and E. S. Krul, Effects of soy protein on lipoprotein lipids and fecal bile acid excretion in men and women with moderate hypercholesterolemia, *J. Clin. Lipidol.*, 2010, **4**, 531–542.
33 N. T. Bendsen, A.-L. Hother, S. K. Jensen, J. K. Lorenzen and A. Astrup, Effect of dairy calcium on fecal fat excretion: a randomized crossover trial, *Int. J. Obes.*, 2008, **32**, 1816–1824.
34 M. A. Denke, M. M. Fox and M. C. Schulte, Short-term dietary calcium fortification increases fecal saturated fat content and reduces serum lipids in men, *J. Nutr.*, 1993, **123**(6), 1047–1053.
35 Y. Shahkhalili, C. Murset, I. Meirim, E. Duruz, S. Guinchard, C. Cavadini and K. Acheson, Calcium supplementation of chocolate: effect on cocoa butter digestibility and blood lipids in humans, *Am. J. Clin. Nutr.*, 2001, **73**(2), 246–252.
36 U. Klinkesorn and D. J. McClements, Impact of lipase, bile salts, and polysaccharides on properties and digestibility of tuna oil multilayer emulsions stabilized by lecithin-chitosan, *Food Biophys.*, 2010, **5**(2), 73–81.
37 K. Molly, M. Vande Woestyne and W. Verstraete, Development of a 5-step multi-chamber reactor as a simulation of the human intestinal microbial ecosystem, *Appl. Microbiol. Biotechnol.*, 1993, **39**(2), 254–258.
38 P. De Boever, R. Wouters, V. Vermeirssen, N. Boon and W. Verstraete, Development of a six-stage culture system for simulating the gastrointestinal microbiota of weaned infants, *Microb. Ecol. Health Dis.*, 2001, **13**(2), 111–123.

39 N. J. Dominy, E. Davoust and M. Minekus, Adaptive function of soil consumption: an *in vitro* study modeling the human stomach and small intestine, *J. Exp. Biol.*, 2004, **207**(2), 319–324.
40 Y. Y. Ji and D. C. Xiao, GIT physicochemical modeling – a critical review, *Int. J. Food Eng.*, 2006, **2**, 4.
41 S. Mun, E. A. Decker and D. J. McClements, Influence of emulsifier type on *in vitro* digestibility of lipid droplets by pancreatic lipase, *Food Res. Int.*, 2007, **40**(6), 770–781.
42 M. Hu, Y. Li, E. A. Decker and D. J. McClements, Role of calcium and calcium-binding agents on the lipase digestibility of emulsified lipids using an *in vitro* digestion model, *Food Hydrocolloids*, 2010, **24**(8), 719–725.
43 Y. Li and D. J. McClements, Inhibition of lipase-catalyzed hydrolysis of emulsified triglyceride oils by low-molecular weight surfactants under simulated gastrointestinal conditions, *Eur. J. Pharm. Biopharm.*, 2011, **79**, 423.
44 M. Brogård, E. Troedsson, K. Thuresson and H. Ljusberg-Wahren, A new standardized lipolysis approach for characterization of emulsions and dispersions, *J. Colloid Interface Sci.*, 2007, **308**, 500–507.
45 B. Borgström and C. Erlanson, Pancreatic juice co-lipase: physiological importance, *Biochim. Biophys. Acta*, 1971, **242**(2), 509–513.
46 H. Lengsfeld, G. Beaumier-Gallon, H. Chahinian, A. De Caro, R. Verger, R. Laugier and F. Carriere, Physiology of Gastrointestinal Lipolysis and Therapeutical Use of Lipases and Digestive Lipase Inhibitors, in *Lipases and Phospholipases in Drug Development*, ed. G. Muller and S. Petry, Wiley, Weinheim, 2004, pp. 195–229.
47 S. J. Rune and K. Viskum, Duodenal pH values in normal controls and in patients with duodenal ulcer, *Gut*, 1969, **10**, 569–571.
48 R. F. Mccloy, G. R. Greenberg and J. H. Baron, Duodenal pH in health and duodenal ulcer disease: effect of a meal, Coca-Cola, smoking, and cimetidine, *Gut*, 1984, **25**, 386–392.
49 M. Armand, P. Borel, P. Ythier, G. Dutot, C. Melin, M. Senft, H. Lafont and D. Lairon, Effects of droplet size, triacylglycerol composition, and calcium on the hydrolysis of complex emulsions by pancreatic lipase: an *in vitro* study, *J. Nutr. Biochem.*, 1992, **3**(7), 333–341.
50 H. Ali, A. Siddiqui and S. Nazzal, The effect of media composition, pH, and formulation excipients on the *in vitro* lipolysis of self-emulsifying drug delivery systems (SEDDS), *J. Dispersion Sci. Technol.*, 2010, **31**(2), 226–232.
51 D. A. Norris and P. J. Sinko, Effect of size, surface charge, and hydrophobicity on the translocation of polystyrene microspheres through gastrointestinal mucin, *J. Appl. Polym. Sci.*, 1997, **63**(11), 1481–1492.
52 I. Bravo-Osunaa, C. Vauthiera, A. Farabollinia, G. F. Palmierib and G. Ponchela, Mucoadhesion mechanism of chitosan and thiolated chitosan-poly(isobutyl cyanoacrylate) core–shell nanoparticles, *Biomaterials*, 2007, **28**, 2233–2243.
53 E. Frohlich and E. Roblegg, Models for oral uptake of nanoparticles in consumer products, *Toxicology*, 2012, **291**, 10–17.
54 A. G. Gaonkar and R. P. Borwankar, Competitive adsorption of monoglycerides and lecithin at the vegetable oil–water interface, *Colloids Surf.*, 1991, **59**, 331.
55 M. Wulff-Pérez, M. J. Gálvez-Ruíz, J. de Vicente and A. Martín-Rodríguez, Delaying lipid digestion through steric surfactant pluronic F68: a novel *in vitro* approach, *Food Res. Int.*, 2010, **43**, 1629.
56 J. S. Patton, P. A. Albertsson, C. Erlanson and B. Borgström, Binding of porcine pancreatic lipase and colipase in the absence of substrate studied by two-phase partition and affinity chromatography, *J. Biol. Chem.*, 1978, **253**, 4195.
57 P. S. Denkova, S. Tcholakova, N. D. Denkov, K. D. Danov, B. Campbell, C. Shawl and D. Kim, Evaluation of the precision of drop-size determination in oil/water emulsions by low-resolution NMR spectroscopy, *Langmuir*, 2004, **20**, 11402.
58 O. Sather, in *Encyclopedic Handbook of Emulsion Technology*, ed. J. Sjöblom, Dekker, New York, 2001, ch. 15.
59 M. C. Carey and O. Hernell, Digestion and absorption of fat, *Semin. Gastrointest. Dis.*, 1992, **3**, 189.
60 D. D. Miller, B. R. Schricker, R. R. Rasmussen and D. Van Campen, An *in vitro* method for estimation of iron availability from meals, *Am. J. Clin. Nutr.*, 1981, **34**, 2248–2256.
61 J. N. Butler, in *Ionic Equilibrium: Solubility and pH Calculations*, Wiley-Interscience, New York, 1998.
62 K. Bauer, L. Gros and W. Sauer, *Thin Layer Chromatography – An Introduction*, Merck, 1991, pp. 61–62.
63 W. Lang, S. Sokhansanj and F. W. Sosulski, Modelling the temperature dependence of kinematic viscosity for refined canola oil, *J. Am. Oil Chem. Soc.*, 1992, **69**, 1054–1055.
64 J. B. Willis, The determination of metals in blood serum by atomic absorption spectroscopy: calcium, *Spectrochim. Acta*, 1960, **16**(3), 259–272.
65 R. Verger, Pancreatic Lipase, in *Lipases*, ed. B. Borgström and H. L. Brockman, Elsevier, Amsterdam, 1984, pp. 84–150.
66 D. I. Watson, A. Smythe, Y. F. Mangnall and A. G. Johnson, Detection of duodenal fluid in the oesophagus with a sodium ion selective electrode, *J. Gastroenterol. Hepatol.*, 1996, **11**, 486.
67 A. Lindahl, A.-L. Ungell, L. Knutson and H. Lennernäs, Characterization of fluids from the stomach and proximal jejunum in men and women, *Pharm. Res.*, 1997, **14**, 497.
68 K. D. Schmidt, P. Abiodun and W. Tolckmitt, Viscosity and electrolyte concentrations in gastric juice from cystic fibrosis children compared to healthy children, *Eur. J. Pediatr.*, 1981, **136**, 193.
69 J. C. Meeroff, J. A. Rofrano and M. Meeroff, Electrolytes of the gastric juice in health and gastroduodenal diseases, *Am. J. Dig. Dis.*, 1973, **18**, 865.
70 J. Lohse and A. Pfeiffer, Duodenal total and ionised calcium secretion in normal subjects, chronic alcoholics, and patients with various stages of chronic alcoholic pancreatitis, *Gut*, 1984, **25**, 874.
71 J. G. Temple, A. Birch and R. Shields, Post-prandial changes in pH and electrolyte concentration, in the upper jejunum after truncal vagotomy and drainage in man, *Gut*, 1975, **16**, 961.
72 L. A. Turnberg and G. Grahame, Secretion of water and electrolytes into the duodenum in normal subjects and in patients with cirrhosis: the response to secretin and pancreozymin, *Gut*, 1974, **15**, 273.
73 E. G. Ball, The composition of pancreatic juice and blood serum as influenced by the injection of inorganic salts, *J. Biol. Chem.*, 1930, **86**, 449.
74 D. C. Whitcomb and G. B. Ermentrout, A mathematical model of the pancreatic duct cell generating high bicarbonate concentrations in pancreatic juice, *Pancreas*, 2004, **29**, e30.
75 Y. Sohma, M. A. Gray, Y. Imai and B. E. Argent, 150 mM $HCO_3(-)$ – how does the pancreas do it? clues from computer modelling of the duct cell, *J. Pancreas*, 2001, **2**, 198.
76 M. Armand, P. Borel, B. Pasquier, C. Dubois, M. Senft, M. Andre, J. Peyrot, J. Salducci and D. Lairon, Physicochemicalcharacteristics of emulsions during fat digestion in human stomach and duodenum, *Am. J. Physiol.*, 1996, **271**, G184.
77 A. Tangerman, A. Van Schaik and E. W. Van der Hoek, Analysis of conjugated and unconjugated bile acids in serum and jejunal fluid of normal subjects, *Clin. Chim. Acta*, 1986, **159**(2), 123–132.
78 S. D. Ladas, P. E. T. Isaacs, G. M. Murphy and G. E. Sladen, Comparison of the effects of medium and long chain triglyceride containing liquid meals on gall bladder and small intestine function in normal man, *Gut*, 1984, **25**(4), 405–411.
79 O. Fausa, Duodenal bile acids after a test meal, *Scand. J. Gastroenterol.*, 1974, **9**(6), 567–570.
80 A. L. Daugherty and R. J. Mrsny, Regulation of the intestinal epithelial paracellular barrier, *Pharm. Sci. Technol. Today*, 1999, **2**, 281.
81 M. Armand, B. Pasquier, M. André, P. Borel, M. Senft, J. Peyrot and J. Salducci, *et al.*, Digestion and absorption of 2 fat emulsions with different droplet sizes in the human digestive tract, *Am. J. Clin. Nutr.*, 1999, **70**, 1096.
82 Z. Vinarov, Y. Petkova, S. Tcholakova, N. Denkov, S. Stoyanov, E. Pelan and A. Lips, Effects of emulsifier charge and concentration on pancreatic lipolysis: 1. in absence of bile salts, *Langmuir*, 2012, **28**, 8127–8139.
83 Z. Vinarov, S. Tcholakova, B. Damyanova, Y. Atanasov, N. Denkov, S. Stoyanov, E. Pelan and A. Lips, Effects of emulsifier charge and concentration on pancreatic lipolysis: 2. interplay of emulsifiers and biles, *Langmuir*, 2012, DOI: 10.1021/la301820w.
84 S. Fernandez, S. Chevrier, N. Ritter, B. Mahler, F. Demarne, F. Carrière and V. Jannin, *In vitro* gastrointestinal lipolysis of four formulations of Piroxicam and Cinnarizine with the self emulsifying excipients Labrasol® and Gelucire® 44/14, *Pharm. Res.*, 2009, **26**, 1901.

85 S. S. Olmsted, J. L. Padgett, A. I. Yudin, K. J. Whaley, T. R. Moench and R. A. Cone, Diffusion of macromolecules and virus-like particles in human cervical mucus, *Biophys. J.*, 2001, **81**, 1930.
86 R. A. Cone, Barrier properties of mucus, *Adv. Drug Delivery Rev.*, 2009, **61**, 75–85.
87 S. K. Lai, Y.-Y. Wang, K. Hida, R. Coned and J. Hanesa, Nanoparticles reveal that human cervicovaginal mucus is riddled with pores larger than viruses, *Proc. Natl. Acad. Sci. U. S. A.*, 2010, **107**, 598.
88 S. K. Lai, D. E. O'Hanlon, S. Harrold, S. T. Man, Y.-Y. Wang, R. Cone and J. Hanes, Rapid transport of large polymeric nanoparticles in fresh undiluted human mucus, *Proc. Natl. Acad. Sci. U. S. A.*, 2007, **104**, 1482.
89 J. Gustafsson, T. Nylander, M. Almgren and H. Ljusberg-Wahren, Phase behavior and aggregate structure in aqueous mixtures of sodium cholate and glycerol monooleate, *J. Colloid Interface Sci.*, 1999, **211**(2), 326–335.
90 D. G. Fatouros, I. Walrand, B. Bergenstahl and A. Müllertz, Colloidal structures in media simulating intestinal fed state conditions with and without lipolysis products, *Pharm. Res.*, 2009, **26**, 361–374.
91 S. Salentinig, L. Sagalowicz, M. E. Leser, C. Tedeschi and O. Glatter, Transitions in the internal structure of lipid droplets during fat digestion, *Soft Matter*, 2011, **7**, 650–661.
92 L. A. Woollett, Y. Wang, D. D. Buckley, L. Yao, S. Chin, N. Granholm, P. J. H. Jones, K. D. R. Setchell, P. Tso and J. E. Heubi, Micellar solubilisation of cholesterol is essential for absorption in humans, *Gut*, 2006, **55**, 197–204.
93 L. Yao, J. E. Heubi, D. D. Buckley, H. Fierra, K. D. R. Setchell, N. A. Granholm, P. Tso, D. Y. Hui and L. A. Woollett, Separation of micelles and vesicles within lumenal aspirates from healthy humans: solubilization of cholesterol after a meal, *J. Lipid Res.*, 2002, **43**, 654–660.
94 G. A. Kossena, B. J. Boyd, C. J. H. Porter and W. N. Charman, Separation and characterization of the colloidal phases produced on digestion of common formulation lipids and assessment of their impact on the apparent solubility of selected poorly water-soluble drugs, *J. Pharm. Sci.*, 2003, **92**, 634–648.

